

Chaos Diagram of Harmonically Excited Vibration Absorber Control Duffing's Oscillator

Salau T.A.O, Ajide O.O.

Abstract— This study utilised positive Lyapunov exponents' criteria to develop chaos diagram on the parameters space of 4-dimensional harmonically excited vibration absorber control Duffing's Oscillator. Relevant simulations were effected by choice combination of constant step Runge-Kutta methods and Gram Schmidt Orthogonal rules. Simulations of 4-dimensional hyper-chaotic models of modified Lorenz and Rösler were used for validation purposes. Lyapunov's spectrums were obtained at (197×301) mesh points of parameters space (μ, α) . Lyapunov's spectrum of modified Lorenz system by constant time step (NRK1) fourth order Runge-Kutta method (0.4208, 0.1650, -0.0807, -26.4603) compare correspondingly well with (0.4254, 0.1286, 0.0000, -26.5493) reported by Yuxia *et al*. Similarly, Lyapunov's spectrum of modified Rösler system by constant time step (NRK1) fourth order Runge-Kutta method (0.1424, 0.0051, -0.0041, -24.0831) compare correspondingly and qualitatively with (0.1287, 0.0149, -0.0056, -22.8617) reported by Marco (1996). The sum of Lyapunov exponents (-22.7237, -31.3107, -27.8797) in Rösler compare correspondingly and qualitatively with variation matrix measure -AVERT (-24.0181, -30.9462, -28.1991) respectively for fourth, fifth and modified fifth order Runge-Kutta methods. The chaos diagram results suggested preferentially higher mass ratio for effective chaos control of Duffing's Oscillator main mass. The parameters space in the region of relative lower mass ratio suffered irregular boundaries. The practical applications of this chaos diagram plot include, by instance, walking in the parameters-space of vibration absorber control Duffing's Oscillator along suitable engineering paths.

Keywords— Chaos Diagram, Vibration Absorber, Duffing Oscillator, Lyapunov exponents, Lorenz and Rösler, Runge-Kutta methods and Gram Schmidt Orthogonal rules

1 INTRODUCTION

CONTROL of chaos relies on the fact that any chaotic attractor contains an infinite number of unstable periodic orbits. Chaos Control can be described as the stabilization, by means of small system perturbations, of one of these unstable periodic orbits (Wikipedia, 2012). The major reason for controlling chaos is to render an otherwise chaotic motion more stable and predictable, which is often highly beneficial in chaos dynamics. The perturbation must be tiny, to avoid significant modification of the system's natural dynamics. Several techniques have been devised for chaos control and numerous research efforts have been made towards chaos control. Experimental control of chaos by one or both of these methods has been achieved in a variety of systems, including turbulent fluids, oscillating chemical reactions, magneto-mechanical oscillators, and cardiac tissues. Sarnobat *et al* (2000) attempt the control of chaotic bubbling with the OGY (ott, Grebogi and Yorke) method and using electrostatic potential as the primary control variable. Andrievskii and Fradkov (2004) carried out a comprehensive review on the problems and methods for control of chaos, which in the last decade was the subject of intensive concern.

It was reported in the review that the applications of chaos in diverse fields such as mechanics (control of pendulums, beams, plates, friction), physics (control of turbulence, lasers, chaos in plasma, and propagation of the dipole domains) as well as in various branches of engineering such as mechanical systems (control of pendulum, beams, plates, vibroformers, microcantilevers, cranes, and vessels), spacecraft, electrical and electronic systems, communication systems, information systems, and chemical and processing industries are enormous. The authors equally stated that the Complexity of the chaotic dynamics gives rise to new problems of control that stimulate further development of the control theory. Control and Chaos for Vibro-Impact and Non-Ideal Oscillators has been examined (Silvio and Ibero, 2008). The authors proposed a satisfactory control procedure which helps in avoiding undesirable behaviour of mechanical systems with practical applications. A dynamics of stability and bifurcation analysis of an asymmetrically nonlinear absorber system that contains a main part and a nonlinear spring was proposed by Chiou-Fong and Chiang-Na. The investigation reveals that the bifurcation sequences illustrate completely the complex phenomena of system dynamics. Furthermore, this study show that the primary bifurcation orbit coexist with orbit of the secondary responses via a saddle-node bifurcation in a specific period excitation range. The results established the fact that a new phenomena occur in a strongly nonlinear system. The phenomenon of ideal synchronization of a pair of identical dynamical systems coupled by a one-to-one negative feedback mechanism is described and explained by Synchronization of two chaotic oscillators via a negative feedback mechanism

- Dr. Salau is currently a Senior lecturer in the Department of Mechanical Engineering, University of Ibadan, Nigeria.
GSM: +2348028644815 E-Mail: tao.salau@mail.ui.edu.ng
- Engr. Ajide is currently a lecturer in the Department of Mechanical Engineering, University of Ibadan, Nigeria.
GSM: +2348062687126 E-mail: ooe.ajide@mail.ui.edu.ng

(Andrzel and Tomasz, 2003). A nonlinear energy sink (NES) that is characterized by its ability to passively realize targeted energy transfer as well as multimodal damping has been examined by Vigié and Kerschen (2009). The perspective of dealing with MDOF linear primary structures requires the development of an efficient NES design procedure. The author proposes the basis of such a procedure based upon the bifurcation analysis of a system composed of a linear oscillator coupled to a NES, using the software MatCont. In the Ashraf et al (2004) paper, the dynamics of a forced Duffing oscillator has been studied by means of modern nonlinear, bifurcation and chaos theories to show that the system is ultimately experiencing chaos. The authors were able to characterize and control this chaotic behavior. A nonlinear recursive Backstepping controller was proposed and the transient performance was also investigated. Simulation results are obtained for the uncontrolled and controlled cases, validating the effectiveness of the proposed controller. The effect of random phase for Duffing-Holmes equation has been investigated (Longsoo, 2011). It was demonstrated that as the intensity of random noise properly increases, the chaotic dynamical behaviour will be suppressed by the criterion of top Lyapunov exponent, which is computed based on the Khasminskii's formulation and the extension of Wedig's algorithm for linear stochastic systems. The obtained results were further validated by the Poincaré map analysis, phase plot, and time evolution on dynamical behaviour of the system, such as stability, bifurcation, and chaos. It can be inferred from this study that the random phase is the most important tool for Suppressing chaos as a nonfeedback control method Efforts has been made to study the dynamics and chaos control of a non-linear electromagnetic seismometer system consisting of an extended Duffing electrical oscillator magnetically coupled with a natural Duffing mechanical oscillator (Sihem et al, 2006). Some bifurcation structures and the variation of the corresponding Lyapunov exponent are obtained in the study. The results obtained showed that transitions from a regular behaviour to chaotic orbits occur for large amplitudes of the external excitation. The application of a simple adaptive damping feedback controller to eliminate the chaotic behaviour in a controlled extended Duffing system was equally examined in order to regulate the chaotic motion of the electromagnetic seismometer system around less complex attractors, such as equilibrium points and periodic orbits. The effectiveness and efficiency of the proposed feedback control strategy was illustrated by means of numerical simulations. A robust control scheme for a class of uncertain chaotic systems in the canonical form, with unknown nonlinearities has been presented by Samuel and Kakmeni (2003). To cope with the uncertainties, the authors combined Lyapunov methodology with observer design. The proposed strategy comprises an exponential linearizing feedback and an uncertainty estimator. The developed control scheme allows chaos suppression. According to the authors, the advantage of this method over the existing results is that the control time is explicitly computed. Simulations studies were conducted to verify the effectiveness of the scheme.

The dearth of literatures which characterizes the parameters space of 4-dimensional harmonically excited vibration ab-

sorber control Duffing's Oscillator using chaos diagram is a strong motivation for this work. This paper employed positive Lyapunov exponents' criteria in developing chaos diagram for this Duffing oscillator dynamics.

2 METHODOLOGY

2.1 Equations of Motions: Harmonically excited and Vibration absorber control Duffing Oscillator

The detail physical model and nomenclatures regarding second order differential nonlinear equations (1) and (2) can be found in Narayanan and Jayaraman (1989) and Dolire and Salau (2012). The dynamics of main mass (M) and Absorber mass (m) are captured respectively with variables x and y relative to corresponding datum.

$$\ddot{x} + \frac{c}{M} \dot{x} - \frac{k}{M} x + \frac{k_c}{M} x^3 + \frac{k_a}{M} (x - y) = \frac{F_o}{M} \sin(\omega t) \quad (1)$$

$$\ddot{y} + \frac{k_a}{m} (y - x) = 0 \quad (2)$$

Introducing the non-dimensional time $\tau = \omega t$ equations (1) and (2) can be expressed in state space form as in equations (3) to (6).

$$\dot{x}_1 = x_2 \quad (3)$$

$$\dot{x}_2 = P_o \sin(\tau) - \beta x_2 + \alpha_1 x_1 - \alpha_c x_1^3 - \alpha_2 (x_1 - x_3) \quad (4)$$

$$\dot{x}_3 = x_4 \quad (5)$$

$$\dot{x}_4 = -\alpha_a (x_3 - x_1) \quad (6)$$

Note that in equations (3) to (6), the state space for the main and absorber masses are represented respectively by (x_1, x_2) and (x_3, x_4) .

$$\text{Similarly we have } P_o = \frac{F_o}{M\omega^2}, \beta = \frac{c}{M\omega}, \alpha_1 = \frac{k}{M\omega^2},$$

$$\alpha_c = \frac{k_c}{M\omega^2}, \alpha_2 = \frac{k_a}{M\omega^2} \text{ and } \alpha_a = \frac{k_a}{m\omega^2}. \text{ It is also}$$

possible to express α_2 in term of mass ratio ($\mu = \frac{m}{M}$)

and α_a in which case $\alpha_2 = \frac{k_a}{M\omega^2} = \frac{m}{M} \frac{k_a}{m\omega^2} = \mu\alpha_a$. The present study characterized the coordinates of parameters plane (μ versus α_a) as either chaotic or not using the estimated positive Lyapunov exponent of the main mass computed by Gram Schmidt Orthogonal rules. Salau and Ajide (2012) refers, the variation matrix (A) for the vibration absorber control Duffing oscillator given by equations (3) to (6) is given by matrix equation (7).

$$A = \begin{pmatrix} 0 & 1 & 0 & 0 \\ (\alpha_1 - 3\alpha_c x_1^2 - \alpha_2) & -\beta & \alpha_2 & 0 \\ 0 & 0 & 0 & 1 \\ \alpha_a & 0 & -\alpha_a & 0 \end{pmatrix} \quad (7)$$

According to Michael (2000) as well as Salau and Ajide (2012), Lyapunov's spectrum must sum to the trace of A (- β).

2.2 Modified Lorenz Model by Yuxia *et al*:

Yuxia Li *et al* (2005) proposed hyper-chaotic system with two nonlinear terms described by equations (8) to (11). This is a 4-dimensional system and a modified form of Lorenz equations studied by Salau and Ajide (2012). Its 4-dimensions make it a good model choice for algorithms validation in the present study. The one to one corresponding state space variables are respectively x , y , z , and w .

$$x = \beta_1 x + \beta_2 y \quad (8)$$

$$y = \beta_3 x + \beta_4 y + w - xz \quad (9)$$

$$z = \beta_5 z + xy \quad (10)$$

$$w = -\beta_k x \quad (11)$$

The corresponding variation matrix (A) for system of equations (8) to (11) is given by equation (12)

$$A = \begin{pmatrix} \beta_1 & \beta_2 & 0 & 0 \\ (\beta_3 - z) & \beta_4 & -x & 1 \\ y & x & \beta_5 & 0 \\ -\beta_k & 0 & 0 & 0 \end{pmatrix} \quad (12)$$

According to Michael (2000) as well as Salau and Ajide (2012), Lyapunov's spectrum must sum to the trace of A ($\beta_1 + \beta_4 + \beta_5$).

2.3 Modified Rösler Model by Rösler:

Addison (1997) as well as Ping and Rui Ding (2011) refers, Rösler proposed hyper-chaotic system with only one nonlinear term described by equations (13) to (16) which is a modified form of Rösler chemical reaction model, see Salau and Ajide (2012). The 4-dimensional forms of this model make it a good choice for algorithms validation in the present study. The one to one corresponding state space variables are respectively x , y , z , and w .

$$\dot{x} = -y - z \quad (13)$$

$$\dot{y} = x + \alpha_{r1} y + w \quad (14)$$

$$\dot{z} = \alpha_{r2} + xz \quad (15)$$

$$\dot{w} = \alpha_{r3} z + \alpha_{r4} w \quad (16)$$

The corresponding variation matrix (A) for system of equations (13) to (16) is given by equation (17).

$$A = \begin{pmatrix} 0 & -1 & -1 & 0 \\ 1 & \alpha_{r1} & 0 & 1 \\ z & 0 & x & 0 \\ 0 & 0 & \alpha_{r3} & \alpha_{r4} \end{pmatrix} \quad (17)$$

According to Salau and Ajide (2012), Lyapunov's spectrum must sum to the average of trace of A over large N-iterations

$$\left(\frac{1}{N} \sum_{i=1}^N (\alpha_{r1} + x_i + \alpha_{r4}) \right).$$

This measure quantity was here tagged AVERT.

2.4 Driven Parameters and Initial Conditions Setting

Common to all studied cases is constant time step ($\Delta t = 0.02$) and Lyapunov's exponent's estimation reset period (i.e. $\tau = \text{LEERP}$) equal $(10 \Delta t)$. For Case-I and Case-II transient period and steady solution periods are respectively $(1000 \Delta t)$ and $(10000 \Delta t)$. For case-III transient and steady solution periods $(10T, 10T)$ and $(50T, 30T)$ were investigated for T equal excitation period ($T = 2\pi$ seconds). For Case-I and Case-III initial conditions (x_1, x_2, x_3, x_4) was set at $(1, 0, 0, 0)$ and for Case-II was set at $(-10, -14, 0.3, 29)$ recommended by Marco Sandri (1996). However the initial conditions for Lyapunov's spectrum estimate for all cases are $(1, 0, 0, 0)$, $(0, 1, 0, 0)$, $(0, 0, 1, 0)$ and $(0, 0, 0, 1)$ in $x_1, x_2, x_3,$ and x_4 -directions respectively.

2.5 Modified Lorenz Model by Yuxia et al: (Case-I)

One set of the driven parameters utilised by Yuxia et al (2005) are $\beta_1 = -\beta_2 = -35, \beta_3 = 7, \beta_4 = 12$ and $\beta_k = 20$ with corresponding Lyapunov's spectrum

$$(\lambda_1 = 0.4254, \lambda_2 = 0.1286, \lambda_3 = 0, \lambda_4 = -26.5493).$$

This case was verified as part validation of the present study algorithms.

2.6 Modified Rösler Model by Rösler: (Case-II)

Driven parameters setting are, $\alpha_{r1} = 0.25, \alpha_{r2} = 3.0, \alpha_{r3} = -0.5$ and $\alpha_{r4} = 0.05$, and for algorithms validation purpose. The corresponding Lyapunov's spectrum $(0.1287, 0.0149, -0.0056, -22.8617)$ was reported by Marco Sandri (1996).

2.7 Harmonically excited and Vibration absorber control Duffing's Oscillator: (Case-III)

Narayanan and Jayaraman (1989) recommended that combination of;

$$P_0 = 0.21, \omega = 1.0, \beta = 0.168, \alpha_1 = \alpha_c = 0.5$$

It is ensured that chaotic response of the main mass and that some appropriate selected α_a will rendered the chaotic

response periodic. However the appropriate mass ratio used was conspicuously missing. The focus of the present study therefore is characterization of the coordinates of plane (μ versus α_a) as either chaotic or not using the estimated positive Lyapunov exponent of the main mass computed by Gram Schmidt Orthogonal rules. The studied plane is $0.01 \leq \mu \leq 0.99$ versus $1.0 \leq \alpha_a \leq 3.0$ with both variable axes traversed respectively at constant step of 0.005 and 0.01.

2.8 Solutions Algorithms

The transients and steady solutions of the models (Case-I, Case-II and Case-III) rate equations and the corresponding Lyapunov's spectrum rate equations were sought for numerically and simultaneously using constant time step fourth, fifth and Butcher's (1964) modified fifth order Runge-Kutta methods. The details of Gram Schmidt Orthogonal rules can be obtained in Marco (1996). The three Runge-Kutta methods are tagged respectively RK4, RK5 and RK5B. The two time stepping systems are tagged NRK1 and NRK2 respectively for constant one full time step and two half-steps in one time step.

3 RESULTS AND DISCUSSION

Lyapunov's spectrum report by Yuxia et al (2005) refers. Table 1 and 2 gives algorithms validation results.

Table 1: Lyapunov's spectrum of Case-I using fourth order, fifth order and Butcher's modified fifth order Runge-Kutta methods and NRK1

	Lyapunov's spectrum				Relative Percentage Absolute Errors		
	Yuxia et al (Actual)	RK4	RK5	RK5B	RK4	RK5	RK5B
λ_1	0.4254	0.4208	0.4263	0.4017	1.1	0.2	5.6
λ_2	0.1286	0.1650	0.1013	0.2014	28.3	21.2	56.6
λ_3	0.0000	-0.0807	-0.0186	-0.0087	UD	UD	UD
λ_4	-26.5493	26.4603	26.5107	26.5933	0.3	0.1	0.2
Trace(A)	-	-	-	-	0.2	0.0	0.0

Note that UD =undefined.

Table 2: Lyapunov's spectrum of Case-I using fourth order, fifth order and Butcher's modified fifth order Runge-Kutta methods and NRK2

Lyapunov's spectrum					Relative Percentage Absolute Errors		
	Yuxia et al (Actual)	RK4	RK5	RK5B	RK4	RK5	RK5B
λ_1	0.4254	0.4210	0.3967	0.3940	1.0	6.7	7.4
λ_2	0.1286	0.1498	0.2011	0.1825	16.5	56.4	41.9
λ_3	0.0000	0.0129	-0.0203	-0.0208	UD	UD	UD
λ_4	-	-	-	-	-	-	-
Trace(A)	25.9953	-25.9549	26.0018	25.9989	0.2	0.0	0.0

Note that UD =undefined

Tables 1 and 2 refers, the relative percentage absolute errors decreases averagely for all Runge-Kutta methods changing time step system from NRK1 to NRK2. Though the highest recorded relative percentage absolute error was 56.60 at RK5B versus NRK1, the overall Lyapunov's spectrum actual variation falls within acceptability level in particular at NRK2 for all computation methods. Each of the Runge-Kutta method recommended average of two positive and two negative Lyapunov's exponents at NRK1 and NRK2 respectively. The trace of A (trace (A)) recorded zero and 0.2 relative percentage absolute error for methods (RK5 and RK5B) and RK4 respectively over the two time step systems.

Table 3: Lyapunov's spectrum of Case-II using fourth order, fifth order and Butcher's modified fifth order Runge-Kutta methods and NRK

Lyapunov's spectrum					Relative Percentage Absolute Errors		
	Marco Sandri (Actual)	RK4	RK5	RK5B	RK4	RK5	RK5B
λ_1	0.1424	0.1287	0.1223	0.1356	9.6	14.1	4.8
λ_2	0.0051	0.0149	-0.0124	-0.0029	192.2	343.1	156.9
λ_3	-0.0041	-0.0056	-0.0226	-0.0098	36.6	451.2	139.0
λ_4	24.0831	22.8617	31.3980	28.0026	5.1	30.4	16.3
Trace(A)	23.9397	22.7237	31.3107	27.8797	5.1	30.8	16.5
AVERT	NA	24.0181	30.9462	28.1991			

Note that NA = Not available

Referring to table 3 , the range of relative percentage absolute error for all quantities of interest and for RK4, RK5 and RK5B are respectively (5.1 - 192.2), (14.1 - 451.2) and (4.8 -156.9). The actual quantities of interest variation relative to available actual values are within acceptable numerical limits. The Trace (A) and AVERT compare very well for all methods (RK4, RK5 and RK5B).

Table 4: Lyapunov's spectrum of Case-II using fourth order, fifth order and Butcher's modified fifth order Runge-Kutta methods and NRK2

Lyapunov's spectrum					Relative Percentage Absolute Errors		
	Marco Sandri (Actual)	RK4	RK5	RK5B	RK4	RK5	RK5B
λ_1	0.1424	0.1133	0.1183	0.1274	20.4	16.9	10.5
λ_2	0.0051	0.0177	0.0088	0.0001	247.1	72.5	98.0
λ_3	-0.0041	0.0015	-0.0146	-0.0098	136.6	256.1	139.0
λ_4	24.0831	25.4754	27.9780	27.8727	5.8	16.2	15.7
Trace(A)	23.9397	25.3429	27.8655	27.7550	5.9	16.4	15.9
AVERT	NA	27.3377	27.6188	28.0735			

Note that NA = Not available

Referring to table 4, the range of relative percentage absolute error for all quantities of interest and for RK4, RK5 and RK5B are respectively (5.9 - 247.1), (16.2 - 256.1) and (10.5 -129.0). The actual quantities of interest variation relative to available actual values are within acceptable numerical limits. The Trace (A) and AVERT compare very well for all methods (RK4, RK5 and RK5B).



Figure 1: Variation of AVERT with number of steady iteration in hyper-chaos of Rösler using fourth order, fifth order and Butcher's modified fifth order Runge-Kutta methods and NRK1

Figure 1 refers, the average AVERT value gravitate towards stable value across methods and with increasing number of steady iteration. This observation agreed with submission of Salau and Ajide (2012) regarding the trace of matrix (A) that are dependent on position variable on attractor of interest (here the hyper-chaos of Rösler). Furthermore, the trends of AVERT variation for the three methods compare very well at lower number of steady iteration, however with increasing iteration number RK4 shows significant deviation from the trend of RK5 and RK5B. Background theoretical and computation knowledge from successful execution of case-I and case-II enables the characterization of the coordinates of parameters plane (μ versus α_a) in case-III as either chaotic or not using the estimated positive Lyapunov exponent of the main mass computed by Gram Schmidt Orthogonal rules. The results obtained are given in tables 5 and 6, and chaos diagram in figures 2 and 3 setting μ as mass ratio and α_a as ALPHA A.

Table 5 : Lyapunov's Spectrum of the Vibration Absorber Control Duffing Oscillator at $\mu = 0.02$, $\alpha_a = 1.27$, NRK1 and NRK2.

Lyapunov's Spectrum	NRK1			NRK2		
	RK4	RK5	RK5B	RK4	RK5	RK5B
λ_1	0.0157	0.0157	0.0157	0.0157	0.0157	0.0157
λ_2	-0.0189	-0.0189	-0.0189	-0.0189	-0.0189	-0.0189
λ_3	-0.0339	-0.0339	-0.0339	-0.0339	-0.0339	-0.0339
λ_4	-0.1309	-0.1309	-0.1309	-0.1309	-0.1309	-0.1309
Trace(A) $= \sum_{i=1}^4 \lambda_i$	-0.1680	-0.1680	-0.1680	-0.1680	-0.1680	-0.1680

Referring table 5, the Lyapunov's spectrum result is the same for all methods regardless of time step systems (NRK1 and NRK2). Likewise the trace (A) = $\sum_{i=1}^4 \lambda_i$ is equal to -0.168 (β - the damp coefficient) across methods and time step systems.

Table 6 : Sample Results of Lyapunov's Spectrum over smooth variation of μ and α_a at constant step of 0.005 and 0.01 respectively and for NRK2

Mass ratio (μ)	ALPHA A (α_a)	Lyapunov's spectrum				Trace (A) $= \sum_{i=1}^4 \lambda_i$
		λ_1	λ_2	λ_3	λ_4	
0.02	1.08	-0.0100	0.0025	-0.0831	-0.0774	-0.1680
0.02	1.09	-0.0089	0.0101	-0.0791	-0.0901	-0.1680
0.02	1.10	-0.0200	0.0162	-0.0828	-0.0813	-0.1679
0.02	1.11	-0.0215	0.0019	-0.0715	-0.0768	-0.1679
0.02	1.12	0.0001	-0.0026	-0.0748	-0.0907	-0.1680
0.02	1.13	0.0102	0.0054	-0.0850	-0.0986	-0.1680
0.02	1.14	0.0121	0.0127	-0.0940	-0.0989	-0.1681
0.02	1.15	0.0082	0.0209	-0.1004	-0.0966	-0.1679
0.02	1.16	0.0008	0.0290	-0.1032	-0.0947	-0.1681
0.02	1.17	-0.0028	0.0308	-0.1061	-0.0898	-0.1679
0.02	1.18	-0.0013	0.0244	-0.1150	-0.0761	-0.1680
0.02	1.19	0.0010	0.0135	-0.0867	-0.0959	-0.1681
0.02	1.20	0.0039	-0.0059	-0.0646	-0.1015	-0.1681
0.02	1.21	0.0055	-0.0153	-0.0702	-0.0880	-0.1680
0.02	1.22	0.0037	-0.0196	-0.0725	-0.0796	-0.1680
0.02	1.23	0.0015	-0.0208	-0.0516	-0.0971	-0.1680
0.02	1.24	0.0052	-0.0355	-0.0595	-0.0782	-0.1680
0.02	1.25	0.0140	-0.0101	-0.0634	-0.1085	-0.1680
0.02	1.26	0.0175	-0.0134	-0.0370	-0.1350	-0.1679
0.02	1.27	0.0157	-0.0189	-0.0339	-0.1309	-0.1680

Referring table 6 either λ_1 or λ_2 is greater than zero for combination of μ and α_a to be listed as not guarantee the control of chaotic response of the main mass in Duffing oscillator. The trace (A) = $\sum_{i=1}^4 \lambda_i$ is equal to -0.1680 (β - the damp coefficient) across the variation of μ and α_a .

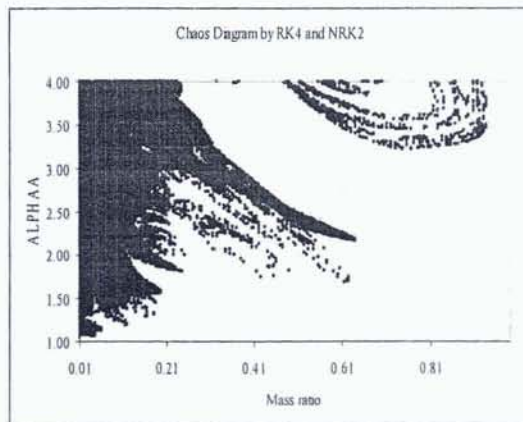


Figure 2: Chaos Diagram of the Main Mass in Vibration Absorber of Harmonically Excited Duffing's Oscillator (10T, 10T)

Figure 2 refers the parameters at the black regions cannot effect chaos control, but chaos control possible with parameters at the blank regions. The chaos diagram suggested preferentially higher mass ratio for effective chaos control of Duffing's Oscillator main mass. However, the appropriate engineering involves cautious selection of main mass chaos control parameters in the region of relatively lower mass ratio that suffered irregular boundaries. Furthermore, similar quantitative and qualitative chaos diagram were obtained using fifth and modified fifth order Runge Kutta methods. Each chaos diagram contains respectively 12535, 12533, 12533 mesh points for RK4, RK5 and RK5B.

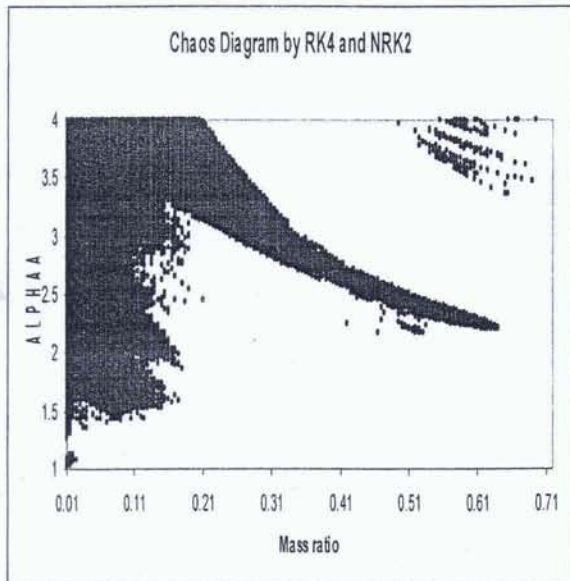


Figure 3: Chaos Diagram of the Main Mass in Vibration Absorber of Harmonically Excited Duffing Oscillator (50T, 30T).

Figure 3 is qualitatively the same as figure 2. The quantitative difference is due to relative larger transient and steady solutions (50T, 30T) compare with corresponding (10T,10T) in figure 2. The chaos diagram (figure 3) contains 10303 mesh points compare with 12535 in figure 2 and for RK4.

4 CONCLUSIONS

This study validated by preliminary investigations of Lyapunov's spectrum in hyper-chaotic modified 4-dimensional Lorenz and Rösler dynamics models shows that Lyapunov exponent is a very effective dynamics characterising tool and that Gram Schmidt rules cumbersome to implement measure it reliably. The chaos diagram results suggested preferentially higher mass ratio for effective chaos control of Duffing's Oscillator main mass using vibration absorber. Practical engineering application of the chaos diagram will involves cautious selection of main mass chaos control parameters in the region of relatively lower mass ratio that suffered irregular boundaries.

REFERENCES

- [1] Andrievskii B.R. and Fradkov A.L.(2004),Control of Chaos: Methods and Applications.Automation and Remote Control,Vol.65,No.4,pp.505-533
- [2] Andrzej S.,Tomasz K.(2003),Synchronization of two chaotic oscillators via a negative feedback mechanism.International Journal of solids and structures.Vol.40,pp.5175-5185
- [3] Ashraf A.Z., Ahmad M.H. and Mohammed A.Z.(2004),Recursive Backstepping Control of Chaotic Duffing Oscillators. Proceeding of American conference, Boston, Massachusetts, June 30 – July 2, 2004.
- [4] Chiou-Fong C. and Chiang-Nan C.(2003),Dynamics of Asymmetric Nonlinear Vibration Absorber.Journal of Marine Science and technology,Vol.11,No.1,pp.8-19
- [5] Folushola O.D. and T.A.O. Salau (2012), Control of Chaotic Oscillation and Response Characterization in Duffing Oscillator Using Vibration absorber. Accepted for publication in Journal of Mechanical Engineering and Automation (JMEA),Scientific and Academic Publishing,USA
- [6] Longsuo Li (2011),Suppressing Chaos of Duffing-Holmes System using Random Phase.Hindawi Publishing corporation,Mathematical Problems in Engineering,Volume 2011,Article ID 538202, 8 Pages doi:10.1155/2011/538202
- [7] Macro S. (1996),Numerical Calculation of Lyapunov Exponents,The Mathematical Journal,Volume 6,Issue 3,Miler Freeman publications,Pg.78-84
- [8] Michael S.(1996),Lecture Materials on Introduction to Chaos at California Institute of Technology,Last Modified Sunday 26,2000 and downloaded Wednesday 4,2012
- [9] Narayanan S. and Jayaraman K.(1989),Control of Chaotic Oscillation by Vibration Absorber,ASME design Technical Conference, 12 th Biennial Conference on Mechanical Vibration and Noise,DE 18.5 pp.391-394.
- [10] Paul S.A.(1997),Fractals and Chaos: An Illustrated Course,Institute of Physics Publishing,United Kingdom(UK),ISBN 0 7503 03999 (bbk),pp.133.
- [11] Ping Z. and Rui D.(2011), A Novel hyperchaotic Systems and its Circuit Implementation,Key Engineering Materials,Volume 467-469,pp.321-324.
- [12] Salau T.A.O. and Ajide O.O.(2012), Simulation and Lyapunov's Exponents Characterization of Lorenz and Rösler dynamics.International Journal of Engineering and technology (IJET),UK,Vol.2,No.9,Pg.1543-1550.ISSN:2049-3444
- [13] Samule B. , Moukam F.M. and Kakmeni F.M.M.(2003),Chaos Control and Duration time of a class of uncertain chaotic systems.Physics letters A 316. Pg.206-217, Elsevier.www.sciencedirect.com
- [14] Sarnobat S.U. (2000),Modification,Identification and Control of Chaotic Bubbling Via Electrostatic potential,Master Thsesi,University of Tennessee,Knoxville.
- [15] Sihem A.,Siewe M.S.,Kakmeni F.M.M. and Samuel B.(2006),Slow Flow Solutions and Chaos Control in an Electromagnetic Seismometer System Chaos,Solitons and Fractals ,Volume 29,pp.988-1001,Elsevier. www.elsevier.com/locate/chaos
- [16] Silvo L.T. and Ibere L.C.(2008),Control and Chaos for Vibro-Impact and Non-ideal Oscillators,Journal of Theoretical and Applied Mechanics,Volume 46(3),pp.641-664,Warsaw
- [17] Vigiúé R. and Kerschen G.(2009),Design Procedure of a Nonlinear Vibration Absorber Using Bifurcation Analysis. Proceedings of the

IMAC-XXVII. February 9-12, 2009, Orlando, Florida, USA. © 2009 Society for Experimental Mechanics Inc.

- [18] Wikipedia (2012), Control of Chaos. Wikipedia is a free encyclopedia. Wikipedia is a registered trademark of the Wikipedia Foundation, Inc., a non-profit organization
- [19] Yuxia Li, Wallace K., Tang S. and Guanrong C. (2005), Hyperchaos evolved from the generalized Lorenz Equation. International Journal of Circuit Theory and Applications, Volume 33, pp. 235-251.

UNIVERSITY OF IBADAN LIBRARY